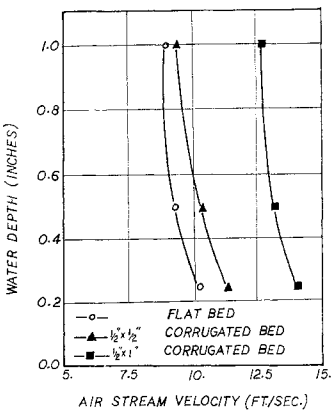

Fig. 4 Dependence of second instability on water depth and bed configurations.

limitation of the frequency response of the wave analyzer, however, only signals down to 5 cps can be detected.

Results and Discussion

The results of the present investigation reveal that there exist two different modes of instabilities of the wind-water interface. The first one occurs at an air velocity of approximately 2.42 fps. The surface waves due to this first instability are of extremely small amplitudes and can be observed visually only by very careful examinations. Furthermore the onset of this instability is found to be independent of the water depth and/or the configuration of the bed. The displayed patterns of the surface waves of the water remain fairly constant after the occurrence of the first critical velocity, except the gradual growth of their amplitudes with increasing speed of the airstream. The surface waves become erratic, however, when the second instability, or "gross instability" as it is called, is reached. The airstream velocities corresponding to this second instability are found to vary from 9.16 to 13.9 fps for different depths of water and different shapes of the bed configuration. This dependence of the second instability on water depth and bed configuration is shown in Fig. 4. The frequency of the water wave at the second instability is found to be approximately 5 cps which corresponds to the highest energy component in the spectrum of the turbulent airstream as shown in Fig. 3.

Conclusion

In conclusion, two different types of instabilities are observed in the present study of wind-wave interaction corresponding approximately to the prediction made by Sontowski[3] et al., Miles,[4–6] and Liang[7] et al. The first instability, occurring at an airstream velocity of 2.42 fps, is found to be independent of the depth of the water and the shape of the bed. The second instability, which gives an erratic wave motion of the water surface, is found to occur at air velocities of 9.16 to 13.9 fps depending on the depth of the water and the shape of the bed. The surface wave at this instability is observed to have a frequency of approximately 5 cps which corresponds to the strongest frequency component in the air turbulence spectrum (see Fig. 3). It suggests clearly, therefore, a one-to-one frequency correspondence for the exchange of energy between the airstream and the water wave at the onset of the second gross instability.

References

[1] Helmholtz, H., "Ueber discontinuirliche Flussigkeitsbewegungen," *Wissenschaftliche Abhandlungen*, J. A. Barth, Leipzig, 1882, pp. 146–157.

[2] Lord Kelvin, "Hydrokinetic Solutions and Observations," "On the Motion of Free Solids through a Liquid," and "Influence of Wind and Capillarity on Waves in Water Supposed Frictionless," Mathematical and Physical Papers, *Hydrodynamics and General Dynamics*, Vol. IV, Cambridge, England, 1910, pp. 69–85.

[3] Sontowski, J. F., Seidel, B. S., and Ames, W. F., "On the Stability of the Flow of a Stratified Gas Over a Liquid," *Quarterly of Applied Mathematics*, Vol. 27, No. 3, 1969, pp. 335–348.

[4] Miles, J. W., "On the Generation of Surface Waves by Shear Flows, Pt. 2," *Journal of Fluid Mechanics*, Vol. 6, No. 4, 1959, pp. 568–582.

[5] Miles, J. W., "On the Generation of Surface Waves by Shear Flows, Part 3, Kelvin-Helmholtz Instability," *Journal of Fluid Mechanics*, Vol. 6, No. 4, 1959, pp. 583–598.

[6] Miles, J. W., "On the Generation of Surface Waves by Shear Flows, Pt. 4," *Journal of Fluid Mechanics*, Vol. 13, No. 3, 1962, pp. 433–448.

[7] Liang, S. S. and Seidel, B. S., "Kelvin-Helmholtz Instability of a Bounded Two-Phase Flow," *Developments in Mechanics*, 11th Midwest Mechanics Conference, Vol. 5, Iowa State Univ., 1969, pp. 135–152.

[8] Gupta, A. K., "An Experimental Investigation of the Generation of Water Waves by Air Shear Flows," TR-116-3, June 1966, Aeroelastic and Structures Research Lab., Massachusetts Institute of Technology, Cambridge, Mass.

[9] Cohen, L. S. and Hanratty, T., "Effect of Waves at a Gas-Liquid Interface on a Turbulent Air Flow," *Journal of Fluid Mechanics*, Vol. 31, Pt. 3, 1967, pp. 467–479.

[10] Davies, J. T., Qidwai, A., and Hameed, A., "Surface Stresses and Ripple Formation Due to Low Velocity Air Passing Over a Water Surface," *Chemical Engineering Science*, Vol. 23, 1968, pp. 331–337.

[11] Wu, J., "Laboratory Studies of Wind-Wave Interactions," *Journal of Fluid Mechanics*, Vol. 34, Pt. 1, 1968, pp. 91–111.

Further Results on Recurrent Lagrange Multipliers for the Low-Thrust Earth-Jupiter Transfer

JACK D. HART* AND W. T. FOWLER†
University of Texas, Austin, Texas

IN Ref. 1, it was shown that some of the initial Lagrange multipliers along with the mission durations for constant power low-thrust Earth-Jupiter transfers are recurrent functions of the launch date. The multipliers which exhibited recurrent behavior were those associated with the motion of the transfer vehicle parallel to the ecliptic plane. The model studied employed inertial rectangular cartesian coordinates to

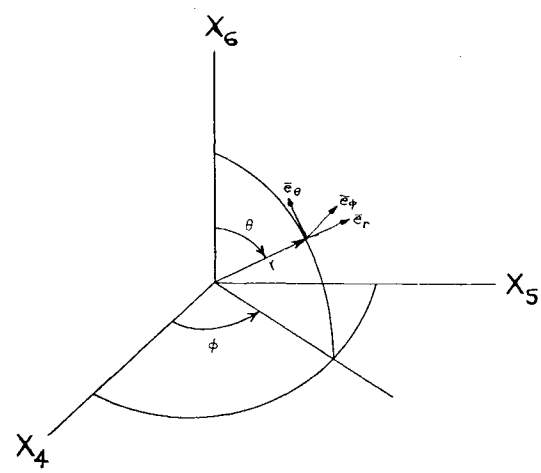

Fig. 1 Spherical coordinate system.

Received May 8, 1970; revision received July 22, 1970. This work was supported under NASA Grant NGR-044-012-008.

* Research Engineer, Department of Aerospace Engineering and Engineering Mechanics.

† Associate Professor, Department of Aerospace Engineering and Engineering Mechanics. Member AIAA.

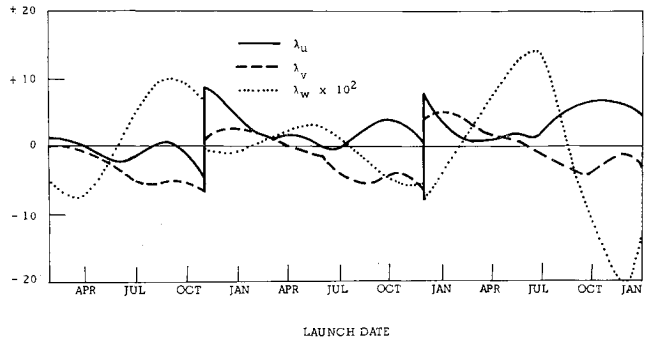

Fig. 2 Lagrange multiplier λ vs launch date.

describe the motion of the vehicle. The orbit of Jupiter was taken to be elliptic and was inclined to the ecliptic plane at the proper angle.

Although the initial optimal Lagrange multipliers were recurrent functions of the launch date, they were not periodic. This lack of periodicity limits the range over which the values of these multipliers can be extrapolated in order to produce optimal trajectories for future launch dates. It was decided to search for a coordinate system in which the initial Lagrange multipliers would be more periodic (and thus more predictable). Spherical polar coordinates, Fig. 1, were found to be such a set of coordinates. The position vector in the new coordinate system is $\bar{r} = r\bar{e}_r$ and the new velocity vector is $\dot{\bar{r}} = \dot{r}\bar{e}_r + rS_\theta\dot{\phi}\bar{e}_\phi + r\dot{\theta}\bar{e}_\theta$.

It was not necessary to reoptimize the trajectories. The optimal initial Lagrange multipliers were transformed in the following manner (see Ref. 2 for details).

Let the coordinate transformation be given by

$$X_j = g_j(x,t) \tag{1}$$

where X_j are the new coordinates and x_j are the old coordinates. Then, the Lagrange multiplier transformation takes the form

$$\Lambda_j = [\partial(g_i^{-1})/\partial X_j]\lambda_i \tag{2}$$

where the Λ_j are the new Lagrange multipliers and the λ_i are the old Lagrange multipliers. The specific transformation relations are as follows:

$$\Lambda_r = S_\theta C_\phi\lambda_u + S_\theta S_\phi\lambda_v + C_\theta\lambda_w \tag{3a}$$

$$\Lambda_\theta = C_\theta C_\phi\lambda_u + C_\theta S_\phi\lambda_v - S_\theta\lambda_w, \tag{3b}$$

$$\Lambda_\phi = -S_\phi\lambda_u + C_\phi\lambda_v \tag{3c}$$

$$\Omega_r = (C_\theta\dot{\theta}C_\phi - S_\theta S_\phi\dot{\phi})\lambda_u + (C_\theta\dot{\theta}S_\phi + S_\theta C_\phi\dot{\phi})\lambda_v - S_\theta\dot{\theta}\lambda_w + S_\theta C_\phi\omega_x + S_\theta S_\phi\omega_y + C_\theta\omega_z \tag{3d}$$

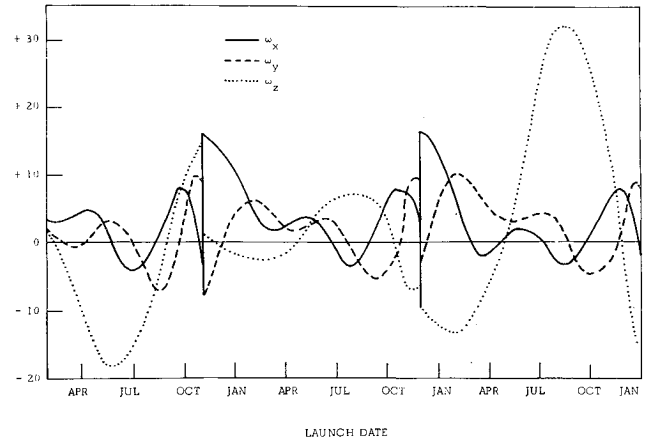

Fig. 3 Lagrange multiplier ω vs launch date.

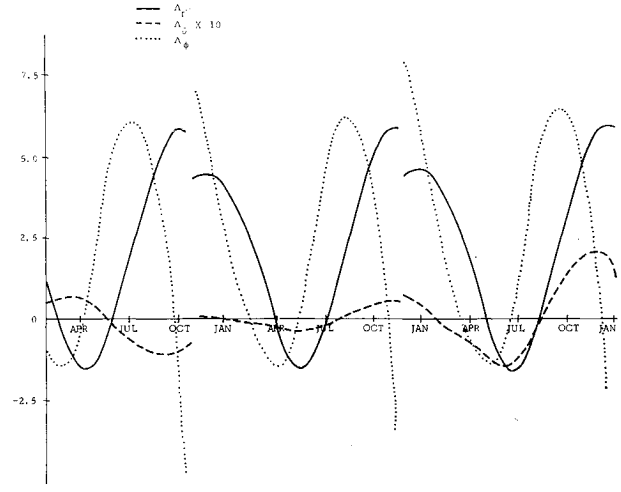

Fig. 4 Lagrange multiplier Λ vs launch date.

$$\Omega_\theta = (\dot{r}C_\theta C_\phi + rS_\theta\dot{\theta}C_\phi - rC_\theta S_\phi\dot{\phi})\lambda_u + (\dot{r}C_\theta S_\phi - rS_\theta\dot{\theta}S_\phi + rC_\theta C_\phi\dot{\phi})\lambda_v + (-\dot{r}S_\theta - rC_\theta\dot{\theta})\lambda_w + rC_\theta C_\phi\omega_x + rC_\theta S_\phi\omega_y - rS_\theta\omega_z \tag{3e}$$

$$\Omega_\phi = (-\dot{r}S_\phi S_\theta - rC_\theta\dot{\theta}S_\phi - rS_\theta C_\phi\dot{\phi})\lambda_u + (\dot{r}S_\theta C_\phi + rC_\theta\dot{\theta}C_\phi - rS_\theta S_\phi\dot{\phi})\lambda_v - rS_\theta S_\phi\omega_x + rS_\theta C_\phi\omega_y \tag{3f}$$

where,

$$\dot{r} = (x_4x_1 + x_5x_2 + x_6x_3)/r$$

$$\dot{\theta} = (x_6\dot{r} - rx_3)/r^2S_\theta$$

$$\dot{\phi} = [rS_\theta x_2 - x_5(\dot{r}S_\theta + rC_\theta\dot{\theta})]/r^2S_\theta^2C_\phi$$

For the spherical polar coordinate system, the multipliers, Λ_r, Λ_θ, and Λ_ϕ orient the thrust vector while the multipliers Ω_r, Ω_θ, and Ω_ϕ are the corresponding negative time rates of change of Λ_r, Λ_θ, and Λ_ϕ respectively.

Figures 2 and 3 (taken from Ref. 1) show the optimal initial Lagrange multipliers in rectangular cartesian coordinates. The transformed (spherical polar) optimal initial multipliers Λ_r, Λ_θ, and Λ_ϕ are given in Fig. 4 while Ω_r, Ω_θ, and Ω_ϕ are given in Fig. 5. The values of the Lagrange multipliers corresponding to the spherical polar coordinates r and ϕ are seen to exhibit near periodic behavior. This near periodic behavior is due to the fact that r and ϕ repeat approximately the same relative configuration every twelve and one-half months. Comparing Fig. 4 with Fig. 2, it is seen that Λ_r and

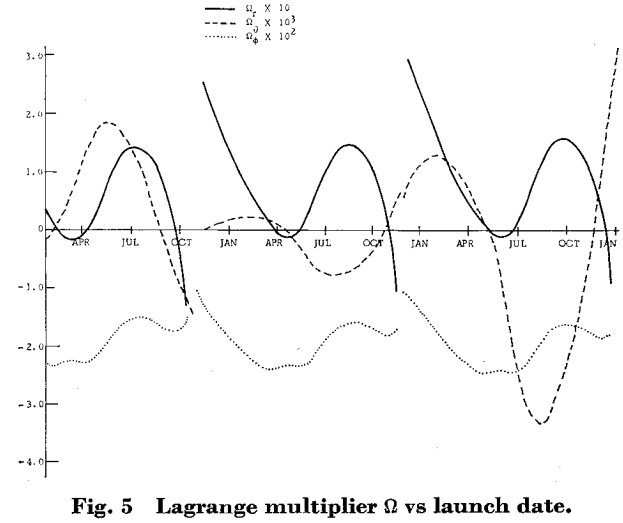

Fig. 5 Lagrange multiplier Ω vs launch date.

Λ_ϕ are more easily predictable than λ_x and λ_y over long periods of time. This is because x and y do not return to the same respective values with any regularity while the values of r and ϕ are approximately periodic. The multipliers corresponding to the movement of Jupiter out of the ecliptic plane in both sets of coordinates (the z and θ multipliers) do not exhibit a periodic behavior over the twelve and one-half month interval.

Thus, the choice of the coordinate system in which the problem is set is quite important when searching for recurrent behavior of the type presented here. It is possible that there is a coordinate system which would exhibit a periodic behavior for all six Lagrange multipliers, but the spherical polar coordinates appear adequate for guessing the initial values of the Lagrange multipliers for launch dates outside the range of values presented.

References

[1] Hart, J. D., Fowler, W. T., and Lewallen, J. M., "Recurrent Nature of Lagrange Multipliers for Optimal Low-Thrust Earth-Jupiter Trajectories," *AIAA Journal*, Vol. 7, No. 7, July 1969, pp. 1357–58.

[2] McDermott, M., Jr., "Comparison of Coordinate Systems for Numerical Computation of Optimal Trajectories," Master's thesis, April 1967, The Univ. of Texas, Austin, Tex.

Nonaffine Similarity Laws Inherent in Newtonian Impact Theory

HOWARD JASLOW*
Technik Inc., Jericho, N. Y.

Nomenclature

C_D, C_L = drag and lift coefficients, respectively
d = body width
k = Newtonian constant
l = body length
$\bar{s}$ = upper limit on s
x, y, s = longitudinal distance, lateral distance, arc length
y' = local slope, dy/dx
θ = angle between local tangent and freestream velocity vector
λ = reference length
ξ = general complementary parameter
$\bar{\xi}$ = upper limit on ξ

Subscripts

0 = basic configuration
1 = complementary configuration
2 = doubly-complementary configuration

NEWTONIAN impact theory provides a basis for studying nonaffine similarity laws; as opposed to affine or linear similarity laws.[1–5] This Note presents those nonaffine similarity laws and transformations for two-dimensional bodies, subject to the limitations of Newtonian impact theory. Considerations are given only to flat-topped bodies at zero angle of attack, since the upper or lower portion of any nonflat-topped configuration can be treated in a similar manner. The similarity laws for complementary configurations are derived from the following Newtonian drag and lift equations

$$C_D = \frac{k}{\lambda}\int_0^d \sin^2\theta\, dy \tag{1}$$

$$C_L = \frac{k}{\lambda}\int_0^l \sin^2\theta\, dx \tag{2}$$

where θ (see Fig. 1) is the angle between the local tangent and the freestream velocity vector (applicable only for $\theta \geq 0$), k is a constant factor ($k = 2$ for the classical Newtonian equation), and λ = reference length.

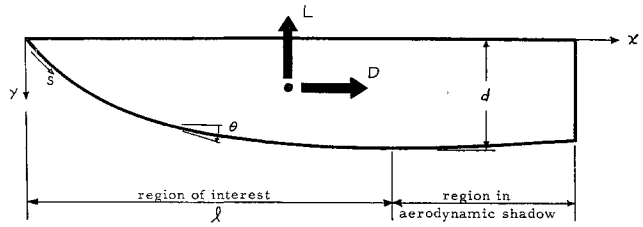

Fig. 1 Flat-topped body.

Definitions of Complementary Configurations

Definition 1: Two configurations are said to be complementary with respect to any parameter ξ if the slopes at corresponding values of ξ have complementary angles; i.e.

$$\theta_0(\xi) + \theta_1(\xi) = \pi/2 \tag{3}$$

Note that this implies that if there is a one-to-one correspondence of θ_0 with ξ, then there is a one-to-one correspondence of θ_1 with ξ. Since $y' \equiv dy/dx = \tan\theta$, it follows from Eq. (3) that

$$y_0'(\xi)\cdot y_1'(\xi) = 1 \tag{4}$$

Definition 2: Transformations effected according to Eqs. (3) or (4) are said to be complementary transformations.

In Fig. 1, only the interval $0 \leq x \leq l$ is of concern. Therefore, only complementary configurations in this interval need be found for the Newtonian application. In other words, two configurations with complementary forebodies and unrelated afterbodies (with the restriction that $\theta < 0$ on the afterbody portion) can have the same similarity properties. These configurations are not completely complementary which gives rise to the need for the following definition.

Definition 3: Two configurations are said to be completely complementary with respect to ξ if both configurations satisfy Eq. (3) and have the same limits in ξ. If the limits overlap, then they are said to be partially complementary.

Another important definition which is used to relate many configurations is as follows.

Definition 4: If a configuration (1) is complementary to a configuration (0) with respect to ξ_1, and if a configuration (2) is complementary to configuration (1) with respect to ξ_2, then it is said that configuration (2) is doubly-complementary to configuration (0) with respect to $\xi_2\xi_1$.

From the previous definitions, it follows that the set of equations

$$y_0'(\xi_1)\cdot y_1'(\xi_1) = 1 \tag{5}$$

$$y_1'(\xi_2)\cdot y_2'(\xi_2) = 1 \tag{6}$$

defines the configurations (0) and (2) as being doubly-complementary with respect to $\xi_2\xi_1$. The extension of this definition to multiply-complementary configurations is obvious. Finally, one last definition related to multiply-complementary configurations is needed.

Definition 5: Two configurations which are related through an even (odd) number of complementary transformations are said to be even (odd)-multiple configurations.

With these definitions, the similarity laws may now be derived. Although the derivations to follow are for the parameters $\xi = x, y$, and s, other ξ parameters may also be used.

Received January 12, 1970; revision received June 15, 1970.
* Chief Analytic Engineer. Member AIAA.